Mem. Fac. Sci. Eng. Shimane Univ.
Series A
32, pp. 19-36 (1998)

Crystal Growth of II–VI and I–III–VI$_2$ Compound Semiconductors by Chemical Transport
2. Thermodynamical Considerations

Yasutoshi NODA

Department of Material Science, Faculty of Science and Engineering, Shimane University
Nishikawatsu 1060, Matsue City, Shimane 690–8504, Japan

Yoshitaka FURUKAWA

Department of Materials Science, Faculty of Engineering, Tohoku University
Aoba-Aramaki, Sendai City, Miyagi 980–8579, Japan

Shigeatsu NAKAZAWA

Department of Metallurgy, Faculty of Engineering, Tohoku University
Aoba-Aramaki, Sendai City, Miyagi 980–8579, Japan

(Received September 18, 1998)

Abstract

Thermodynamical calculations were performed for the chemical transport systems of $ZnSe+I_2$ and $AgGaS_2+X_2$($X=Cl$, Br and I). The vapor pressures of gas molecules were calculated at the source and growth zones by using the thermodynamic data. The transport rates for ZnSe and $AgGaS_2$ were estimated on the basis of the transport equation, which is limited by the diffusion and laminar flow of gaseous molecules and modified by thermal convection at high pressures. The diffusibities of the molecules were estimated by using Lennard-Jones parameters. The calculated transport rates almost reproduced the characteristic features observed for both ZnSe and $AgGaS_2$. In case of ZnSe transport, the abrupt change in the transport rate was attributable to the thermal convection. The transport rate calculated for $AgGaS_2$ reproduced the observed gradual change with an increase of halogen, but did not realize the observed order ($Cl<Br<I$) in the magnitude of the transport rate.

The chalcogen (Se or S) vapor pressures calculated at the growth zone increased with an increase of transport agent and exceeded that of dissociation of the stoichiometric ZnSe or $AgGaS_2$. The fact may have caused the introduction of the non-radiative recombination centers in the grown crystals.

1. Introduction

The chemical transport is one of the most important techniques for crystal growth of the compound semiconductors$^{1)}$.However the exact knowledge on the closed tube crystal growth has hardly been obtained. The transport equation has been proposed for chemical transport in closed system considering diffusion and laminar flow as fundamental transport mechanism²⁾ and the calculation method has been applied to many systems³⁾.

The ZnSe and $AgGaS_2$ crystal growth by chemical transport has been performed in a closed system. The large size ZnSe single crystal was obtained under the optimum growth condition in the vertical transport system by using iodine, where the growth is limited by thermal convection⁴⁾. The transport reactions and the morphologies of the grown crystals were investigated, but the transport mechanism has not been fully analyzed for the ZnSe–I_2 system⁵⁾. Preliminary works for $AgGaS_2$ using iodine as a transport agent have not fully developed the method because of its low growth rate⁶,⁷⁾.

In the authors' previous study⁸⁾, the single crystals of ZnSe and $AgGaS_2$ were grown under a variety of growth conditions using iodine and halides as the transport agent. The transport rate of ZnSe showed a gradual increase, a plateau and a steep increase with an increase of iodine. The transport rate of $AgGaS_2$ was found to exhibit a maximum at some definite amount of transport agent, but the relationship between transport rate and amount of iodine is steep or slow depending upon whether the transport agent is iodine or halide. The maximum transport rate increased in the order of Cl, Br and I in the halides as the transport agent. Thermodynamical calculation will help to clarify transport mechanism.

In the present study, the calculation of the transport rate was performed to analyze the transport and crystal growth mechanism.

2. Calculation for ZnSe–I_2 system

In the calculated closed-tube system, the reaction tube was held horizontally in a furnace of two constant temperature zones, source and growth zones⁸⁾. The calculations were performed as shown in Fig. 1 on the basis of the thermodynamic data and the conventional transport equation²,³⁾.

2.1 Transport reaction of ZnSe–I_2 system

In the ZnSe–I_2 system, the species (i) in the gas phase are assumed to be ZnI_2, Zn, I, I_2 and Se_2. The system involves following three reactions:

$$ZnSe(s) = Zn(g) + 1/2Se_2(g), \tag{1}$$
$$Zn(g) + I_2(g) = ZnI_2(g), \tag{2}$$
$$I_2(g) = 2I(g). \tag{3}$$

The equilibrium constants (K_j) involved in these reactions ($j=1$–3) are expressed in terms of partial pressures (P_i) of the i-th gas component;

$$K_1 = P_{Zn}P_{Se_2}^{1/2}, \tag{4}$$
$$K_2 = P_{ZnI_2}/P_{Zn}P_{I_2}, \tag{5}$$
$$K_3 = P_I^2/P_{I_2}. \tag{6}$$

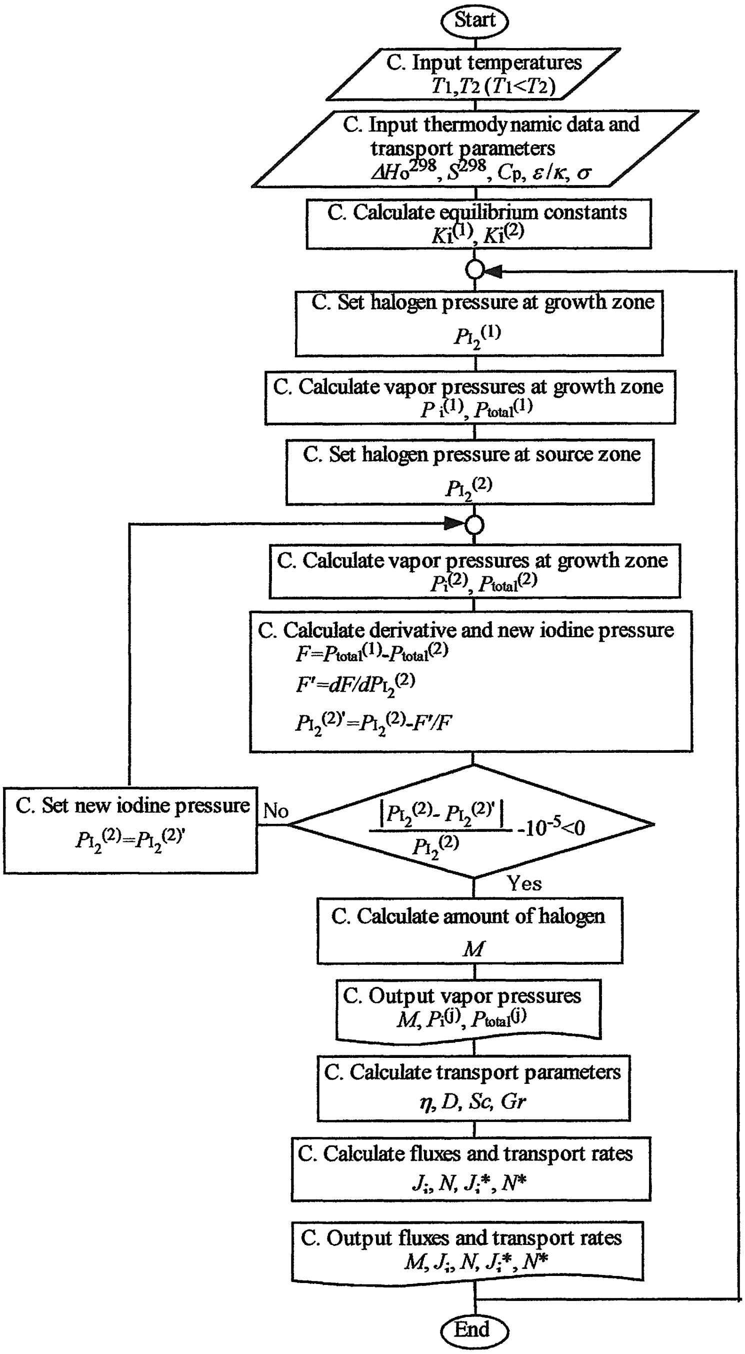

Fig. 1. Thermodynamical calculation for chemical transport.

Table I Thermodynamic data[9,10] and Lennard-Jones parameters[19] for ZnSe–I_2 system.

	ΔH_o^{298} (J/mol)	S_o^{298} [J/(K·mol)]	C_p[J/(K·mol)][a)]			Molecular weight (10^{-3} kg/mol)	σ (mm)	ε/κ (K)	note[b)]
			a	$b\cdot10^3$	$c\cdot10^{-5}$				
ZeSe(s)	−163000	84	50.2	5.77	0.0	144.35	—	—	—
ZnI_2(g)	−89500	300	59.0	0.0	0.0	318.18	0.455	1373	$HgCl_2$
Zn(g)	130000	161	20.8	0.0	0.0	65.37	0.350	1341	Kr
Se_2(g)	139000	244	44.6	−2.66	−2.50	157.92	0.427	1025	Br_2
I_2(g)	62300	260	37.2	0.0	0.0	253.81	0.516	474[c)]	—
I(g)	107000	181	18.6	0.0	0.0	126.90	0.422	289	HI

a) $C_p=a+bT$; cT^{-2}, b) taken from the listed molecule[19].
c) taken from literature[19], although the averaged value of those from T_m and T_b is 637 K.

The K_j's were calculated for the equilibria (1)–(3) using thermodynamic data[9,10] listed in Table I.

For ZnSe to be transported, the following condition of the stoichiometric composition (Zn/Se=1) is given in each zone,

$$P_{Zn}+P_{ZnI_2}=2P_{Se_2}. \tag{7}$$

In the growth zone at T_g, a tentative value of P_{I_2} was assumed and partial pressures (P_i) were calculated from the equations (4)–(7). In the source zone at T_s, P_{I_2} was iterated to refine P_i's so that the total pressure became equal to that at the growth zone. The total amount of iodine charged in the growth ampoule was estimated in Appendix 1. The calculation was performed at T_g=1073~1173 K and ΔT=25~50 K.

The transport rate was evaluated in Appendix 2 by calculating the mean diffusivity of gaseous molecules on the basis of the Lennard-Jones parameters in Appendix 3. Under the condition of high vapor pressure, flux and transport rate were modified by thermal convection[12].

2.2 Calculated results and discussion for ZnSe–I_2 system

Figure 2 shows the relationship between M and P_i, where solid and dashed lines represent the P_i-values at the source (T_s=1098 K) and growth (T_g=1073 K) zones, respectively. It is found that the partial pressures of ZnI_2, I, I_2 and Se_2 monotonously increase with an increase of M. The Zn readily reacts with iodine to form ZnI_2. Thus, the vapor pressure of Zn is less than 10 Pa and does not appear in the figure. The selenium pressure (P_{Se_2}) at the growth zone was 10^4–10^5 Pa in the transport atmosphere, which must be comparable to the dissociation pressure of stoichiometric ZnSe composition to obtain good quality single crystal. The congruent sublimation is given as follows;

$$ZnSe(s)=Zn(g)+1/2Se_2(g). \tag{8}$$

The equilibrium constant for (8) is given by under condition of $P_{Zn}=P_{Se_2}$ as follows;

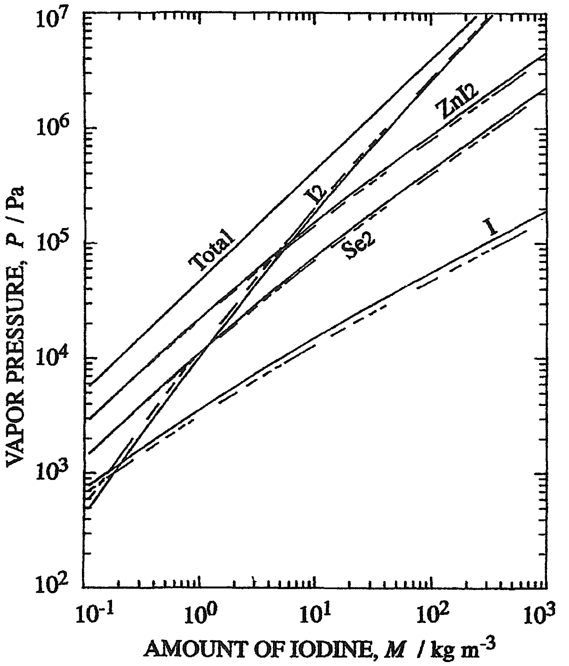

Fig. 2. Vapor pressures of gaseous molecules as a function of amount of iodine, calculated at $T_s=1098$ and $\Delta T=25$ K in the ZnSe+I$_2$ system. Solid line stands for the source zone and dashed line for the growth zone.

$$K=P_{Zn}P_{Se_2}^{1/2}=P_{Se_2}^{3/2}. \tag{9}$$

By using thermodynamic data in Table I, the P_{Se_2} value in (9) amounted to about 1 Pa, which is much less than those in the transport systems. Therefore the excess Se$_2$ pressure may have caused lattice defects and their associations in the crystals resulting predominant nonradiative recombination centers[8].

The calculated gas fluxes including thermal convection are shown in Fig. 3. The transport direction of ZnI$_2$, I and Se$_2$ is forward (from the source to the growth zone), while that of I$_2$ reverse. The result supports the transport reaction[1,5] depending on M as follows,

$$\mathrm{ZnSe(s)+I_2(g)=ZnI_2(g)+1/2Se_2(g)}, \tag{10}$$

which neglects the reaction (3).

The forms of the grown crystals[8] might be related with the gas flux as follows: the fine granular crystals at $M<1.0$ kg/m^3 might be due to the low flux. In the plateau region of $1.0 \leqq M \leqq 5.0$ kg/m^3, the flux seems to become large enough for the growth of the bulk single crystals. The large flux due to the thermal convection at $M>5.0$ kg/m^3 may lead to the needle-like crystals[13]. From these results, the optimum condition of growing large size ZnSe single

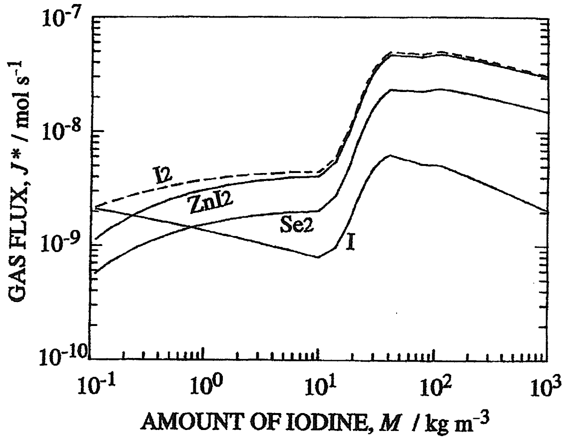

Fig. 3. Fluxes of gaseous molecules as a function of amount of iodine, calculated at $T_s=1098$ K and $\Delta T=25$ K with thermal convection in the ZnSe+I_2 system. Solid line stands for forward transport from source to growth zone and dashed one for backward.

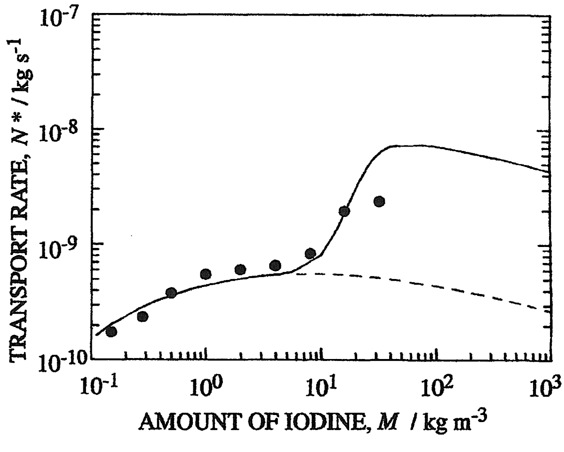

Fig. 4. Transport rate of ZnSe as a function of amount of iodine. The lines were calculated at $T_s=1098$ K and $\Delta T=25$ K with (solid line) and without (dashed line) consideration of thermal convection. The symbol (●) stands for experimental data.

crystals can be sought in the plateau region, where the growth rate of ZnSe crytals was limited by laminar flow and diffusion in the gas phase.

It is remarkable the calculated transport rate is almost along with the observed one as shown in Fig. 4. The solid and dashed lines stand for the transport rates calculated with and without considering thermal convection, respectively. At $M<1.0$ kg/m^3, both of the calculated and observed transport rates show a gradual increase with an increase of M. The calculated transport rate and the observed data form a almost plateau at $M=1.0\sim5.0$ kg/m^3. At $M>5.0$ kg/m^3, the contribution from thermal convection was found to be significant, resulting the steep increase in the transport rate. The transport experiment with $M>40$ kg/m^3 was not performed, since the total vapor pressure of about 1.5×10^6 Pa at $M=40$ kg/m^3 is close to the tolerable limit for the growth quartz ampoule.

Figure 5 shows plots of observed transport rate versus calculated gas flux, which forms a linear relationship for each data set of growth condition. The transport rate do not exceed 10^{-9} kg/s, until the contribution from the thermal convection is significant. It is found that no great difference in the transport rate among the data sets, although the one set at $T_s=1123$ K with $\Delta T=50$ K is separated in gas flux from the others. The fact suggests that the growth rate might be limited by deposition rate as well as by diffusion and laminar flow.

3. Calculation for AgGaS$_2$–X$_2$ systems

3.1 Transport reaction of AgGaS$_2$–X$_2$ system

The calculation was performed as was the case for ZnSe by using the thermodynamic data in the AgGaS$_2$–X$_2$ system where the gas phases were AgX, GaX$_3$, GaX, X, X$_2$ and S$_2$ by using halogen (X=I, Br and Cl) as the transport agent. The systems involve the following three reactions;

$$AgGaS_2(s)+2X_2=AgX(g)+GaX_3(g)+S_2(g), \quad (11)$$
$$GaX_3(g)=GaX(g)+X_2(g), \quad (12)$$
$$X_2(g)=2X(g). \quad (13)$$

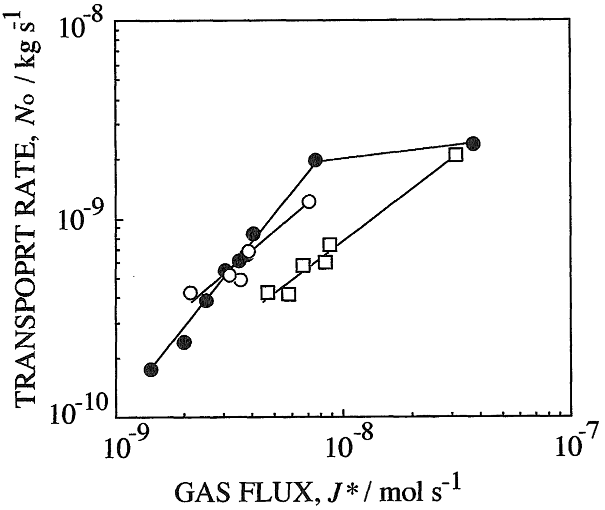

Fig. 5. Plots of observed transport rate versus calculated gas flux of ZnI$_2$ in the ZnSe+I$_2$ system. The growth conditions: (●); $T_s=1098$ K and $\Delta T=25$ K, (○); $T_s=1123$ K and $\Delta T=25$ K and (□); $T_s=1123$ K and $\Delta T=50$ K.

The condensed phase of AgX was not included in the reactions, since the liquid phase was not formed and any indication of the crystal growth from melt was not recognized in the amount of halogen less than 1 kg/m³. The equilibrium constants (K_j) involved in these reactions (j=1–3) are expressed by,

$$K_1=P_{AgX}P_{S_2}/P_{X_2}^2, \tag{14}$$

$$K_2=P_{GaX}P_{X_2}/P_{GaX_3}, \tag{15}$$

$$K_3=P_X^2/P_{X_2}. \tag{16}$$

The conditions of the constant metal atom ratio (Ag/Ga=1) and the stoichiometry condition ((Ag+Ga)/S_2=1) hold in each zone for $AgGaS_2$ to be transported, which are expressed as follows;

$$P_{AgX}=P_{GaX_3}+P_{GaX}, \tag{17}$$

$$P_{AgX}+P_{GaX_3}+P_{GaX}=P_{S_2}. \tag{18}$$

Partial pressures (P_i's) were calculated after the calculation of the K_js from the free energies for the equilibria (1)–(3) using thermodynamic data[9–11] listed in Table II. The total amount of

Table II Thermodynamic data[9–11] and Lennard-Jones parameters[19] for $AgGaS_2$–X_2 system.

	ΔH_0^{298} (J/mol)	S_0^{298} [J/(K·mol)]	C_p[J/(K·mol)][a]			Molecular weight (10^{-3} kg/mol)	σ (mm)	ε/κ (K)	note[b]
			a	$b\cdot10^3$	$c\cdot10^{-5}$				
$AgGaS_2$(s)	−370000	172	69.7	22.6	0.0	241.7	—	—	—
AgCl(g)	100000	246	37.7	0.0	0.0	143.3	0.418	1726	LiI
AgBr(g)	121000	257	37.7	0.0	0.0	187.8	0.424	936	$BeBr_2$
AgI(g)	138000	264	37.7	0.0	0.0	234.8	0.544	430	BBr_3
GaCl(g)	−83700	241	37.7	0.0	0.0	105.2	0.496	188	$CClF_3$
GaBr(g)	−33500	252	37.7	0.0	0.0	149.6	0.418	1726	LiF
GaI(g)	41800	259	37.7	0.0	0.0	196.6	0.424	936	$BeBr_2$
$GaCl_3$(g)	−427000	326	75.4	0.0	0.0	176.1	0.424	936	$BeBr_2$
$GaBr_3$(g)	−301000	362	75.4	0.0	0.0	309.4	0.612	442	CBr_4
GaI_3(g)	−117000	383	75.4	0.0	0.0	450.4	0.563	696	HgI_2
Cl(g)	121000	165	21.0	0.0	0.0	35.5	0.361	131	HgI_2
Br(g)	111000	175	20.9	0.0	0.0	79.9	0.367	237	—
I(g)	107000	181	18.6	0.0	0.0	126.90	0.422	289	—
Cl_2(g)	0	223	36.9	0.06	−2.85	70.9	0.422	316	—
Br_2(g)	30500	245	37.8	0.0	−1.55	159.8	0.430	508	—
I_2(g)	62300	260	37.2	0.0	0.0	253.8	0.516	474	—
S_2(g)	130000	228	35.7	0.28	−3.31	64.1	0.452	847	—
Ag_9GaS_6(s)[c]	−1480000	742	45.3	5.65	0.0	1233.0	—	—	—
Ga_2S(g)	20900	290	56.0	0.275	−9.25	171.5	—	—	—

a) $C_p=a+bT+cT^{-2}$, b) taken from the listed molecule[19].

c) estimated on the basis of the literature[19].

halogen (M) charged in the reaction tube was estimated in Appendix 1 by using partial pressures of all gaseous halides and halogens in both zones.

The flux (J_i) of the i-th gas molecule and the transport rate of AgGaS$_2$ were calculated on the basis of the transport equation in Appendix 2 using the Lennard-Jones parameters in Appendix 3. Under the condition of high vapor pressure, flux and transport rate were modified by thermal convection[12)]. The calculation was performed at T_g of 1173–1273 K and the temperture difference ($\Delta T = T_s - T_g$) of 10–50 K.

3.2 Calculated results and discussion for AgGaS$_2$–I$_2$ system

Figure 6 shows the relationship between M and P_i, where solid and dashed lines represent those at source ($T_s = 1248$ K) and growth ($T_g = 1223$ K) zones, respectively. It is found that the vapor pressures of halides, halogen and sulfur molecules monotonously increase with an increase of M at $M > 10^{-1}$ kg/m^3. Chlorine and bromine are ready to react with Ag and Ga to

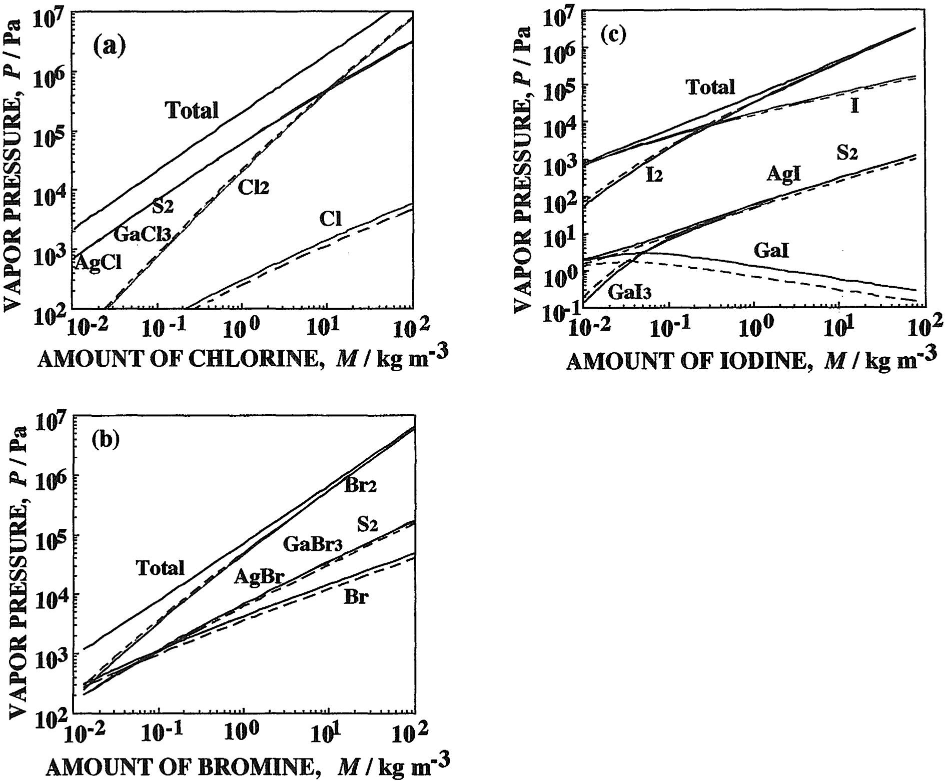

Fig. 6. Plots of vapor pressure versus amount of halogen, calculated at $T_s = 1248$ and $\Delta T = 25$ K in the AgGaS$_2$+X$_2$ systems. Transport agent: (a) Cl, (b) Br and (c) I. Solid line stands for the source zone and dashed line for the growth zone.

form the halide so that the vapor pressures of the halides are larger than those of halogens. On the other hand, the vapor pressures of iodines (I and I_2) are by several orders of magnitude larger than those of the iodides.

The sulfur pressure in Fig. 6c was found to increase with an increased amount of iodine and amounted to about 5×10^1 Pa at $M=10^0$ kg m^{-3} by using iodine. Figure 7 shows plots of emission intensity (I_{Ex}) due to free exciton[8] versus sulfur pressure evaluated from amount of iodine as the transport agent. The sulfur pressures at the growth zone must be close to the dissociation pressure of the stoichiometric $AgGaS_2$, in order to obtain good quality single crystals by chemical transport. The following dissociation of $AgGaS_2$ might be induced from the results of the heat-treatment experiments[14] where Ag_2S-rich Ag_9GaS_6 and Ga_2S_3 deposited;

$$AgGaS_2(s)=1/9Ag_9GaS_6(s)+4/9Ga_2S(g)+4/9S_2(g), \tag{19}$$

The equilibrium constant for the reaction (19) is given under the condition of $P_{Ga_2S}=P_{S_2}$ as follows,

$$K=(P_{Ga_2S}P_{S_2})^{4/9}=P_{S_2}^{8/9}, \tag{20}$$

By using the thermodynamic data listed in the Table II, the P_{S_2} value in (20) amounted to about 10^{-1} Pa. It is noteworthy that P_{S_2} on the chemical transport exceeds that on the dissociation.

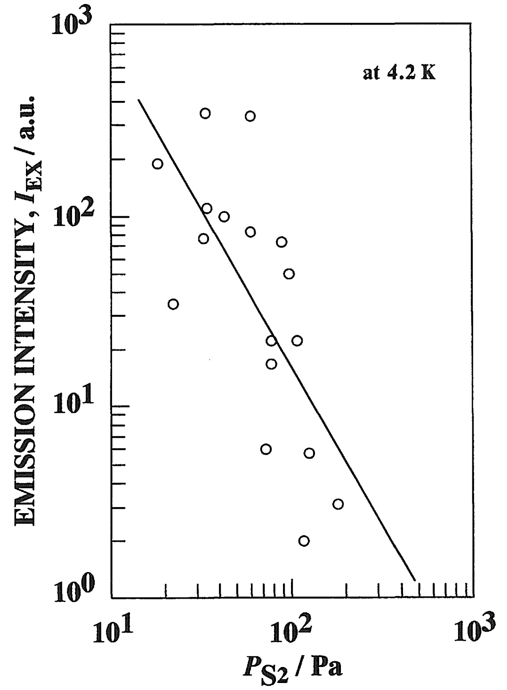

Fig. 7. Plots of observed emission intensity of free exciton versus calculated sulfur pressure in the $AgGaS_2$ $+I_2$ systems. The transport experiment using iodine at $T_g=1173$–1123 K, $\Delta T=10$–50 K.

Therefore the significant decrease of I_{Ex} with an increased amount of iodine indicates that the non-radiative recombination centers and the degradation of the grown crystals might have been caused from such excess sulfur pressure on the chemical transport.

Figure 8 shows the relationship between M and J_i which were calculated by using P_i's in Fig. 6. AgX, GaX, X and S_2 are always forward transported from source to the growth zone (solid line) and while X_2 backward as shown by dashed lines. The thermal convection was significant at large amount of transport agent, where the dotted dashed lines indicate the fluxes without thermal convection. Figure 9 shows plots of the calculated transport rate of $AgGaS_2$ in terms of M. The solid and dashed lines stand for the transport rates calculated with and without considering thermal convection, respectively. The effect of the thermal convection is appreciable as a steep increase of the transport rate at $M > 10^1$ kg/m^3. At $M = 10^{-1} - 10^1$ kg/m^3, the transport rate using bromine and iodine as the transport agent decreases with an increase of M, while the rate increases with an increased amount of chlorine.

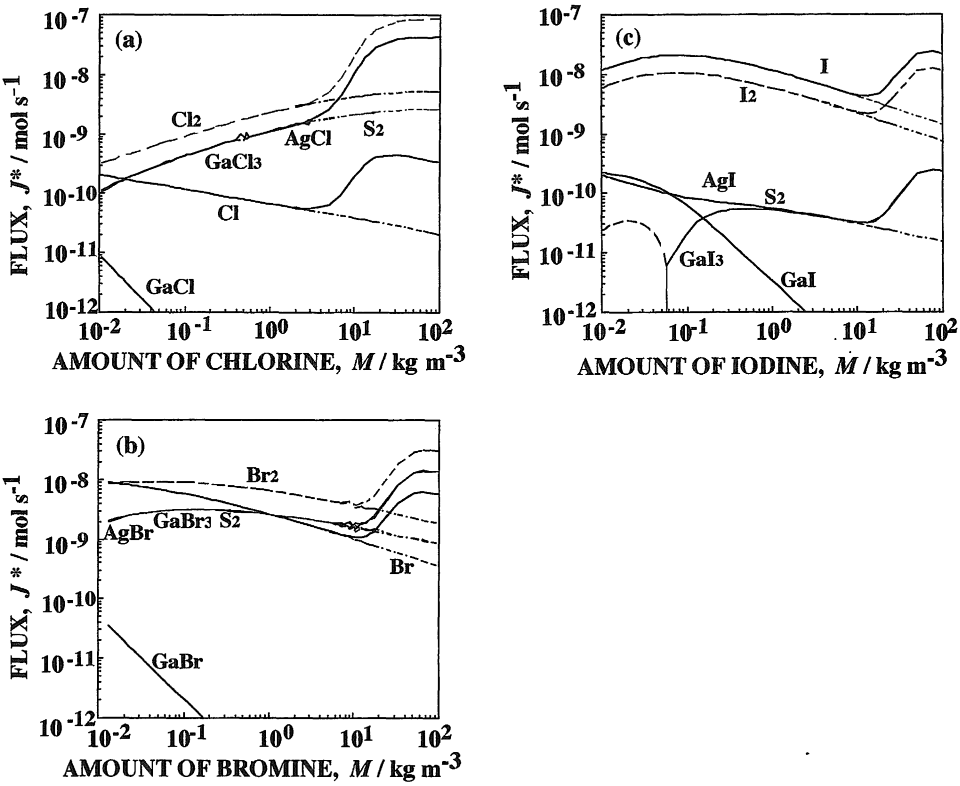

Fig. 8. Fluxes of gaseous molecules as a function of amount of halogen, calculated at $T_s = 1248$ K and $\Delta T = 25$ K under consideration of thermal convection in the $AgGaS_2 + X_2$ systems. Transport agent: (a) Cl, (b) Br and (c) I. Solid line stands for forward transport from source to growth zone and dashed one for backward.

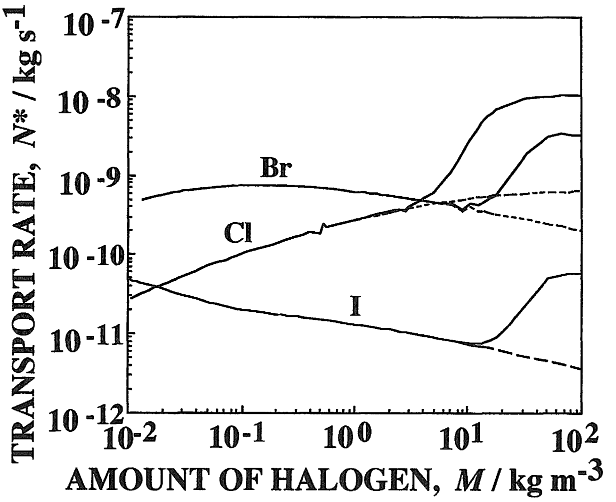

Fig. 9. Calculated transport rate of $AgGaS_2$ as a function of amount of halogen, at $T_s=1248$ K and $\Delta T=25$ K with (solid line) and without (dashed line) consideration of thermal convection.

Figure 10 shows the observed transport rate in terms of M measured by using halide and iodine as the source material of halogen. The transport rate using iodine and iodide was by 10 times larger than those using other halogens. The calculation reproduced the observed gradual decrease in the transport rate at $M=10^0-10^1$ kg/m^3 in the cases of bromine and iodine. The decreased transport rate was observed for AgI (I) and AgBr ($CdBr_2$) with a decrease of M in the region of $M<10^{-1}$ kg/m^3, which might be caused from the process limited by the supply of the gaseous molecules. As for the transport agents, the discrepancy between the observed and calculated transport rates was found to exist in the magnitude. The calculation also did not reproduce the order of $Cl<Br<I$ observed in the transport rate. The order corresponds to that of the enthalpy (ΔH_0^{298}) of Ag and Ga halides listed in Table II. Therefore further thermodynamical considerations including the deposition process might be necessary to clarify the discrepancy.

4. Summary

(1) Thermodynamical calculations were performed for the chemical transport systems of $ZnSe+I_2$ and $AgGaS_2+X_2$ (X=Cl, Br and I). The vapor pressures and the fluxes of the gaseous molecules were calculated. The transport rates of ZnSe and $AgGaS_2$ were estimated on the basis of the transport equation, where the transport is limited by the diffusion and laminar flow of gaseous molecules and the diffusibities of the molecules were estimated by using Lennard-Jones parameters.

(2) The chalcogen vapor pressures (Se_2 in ZnSe or S_2 in $AgGaS_2$) were found to increase with an increase of transport agent. These values at growth zones exceeded those of the dissocia-

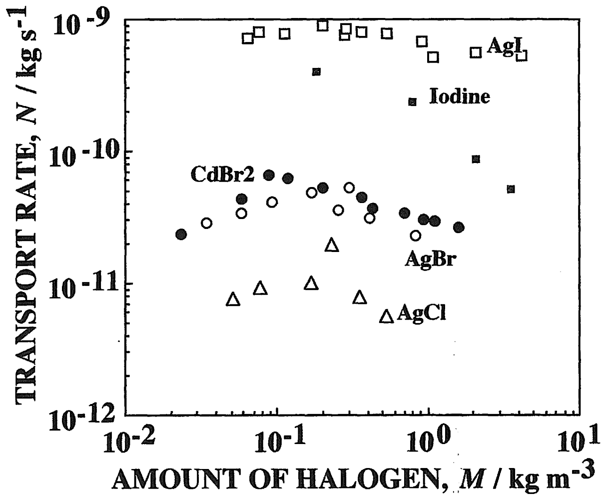

Fig. 10. Observed transport rate of $AgGaS_2$ plotted against amount of halogen, at $T_s=1248$ K and $\Delta T=25$ K by using a variety of halides as the source of transport agent.

tion of the stoichiometric ZnSe or $AgGaS_2$, which might have caused the poor quality by the introduction of non-radiative recombination centers in the grown crystals.

(3) The calculated transport rates for ZnSe was almost along the observed data, which indicates that the transport is limited by diffusion and laminar flow at $M \leqq 5.0$ kg/m^3, while the steep increase at $M > 5.0$ kg/m^3 was due to the thermal convection.

(4) The calculated transport rates for $AgGaS_2$ reproduced the observed gradual change with an increase of halogen, but not realized their magnitudes and the order (Cl<Br<I) in the observed transport rates. Therefore further thermodynamical considerations including the deposition process might be necessary to clarify the discrepancy.

Appendix

1. Amount of transport agent

In these calculations for ZnSe or $AgGaS_2$, the total amount of halogen (M) in the transport agent charged in the growth ampoule was estimated by using partial pressures of all gaseous halides (ZnI_2 or AgI, GaI_3, GaI) and halogens (I and I_2, or X and X_2) in both zones as follows,

$$M(\text{kg/m}^3) = M_x \times 10^{-3} \sum_{i}^{2} \sum_{j}^{n} \frac{1}{RT_i} m_j P_j^{(i)}, \tag{A1}$$

where M_x is the atomic weight of halogen atom, i is source and growth zones, R is gas constant and m_j the number of halogen (X_2) in a molecule of the j-th gas component.

2. Transport equations

The transport equation was proposed on the assumption that one-dimensional diffusion and laminar flow limit the transport from the source to the growth zone. The flux (J_i) of i-th gas component is given by

$$J_i(\mathrm{mol/s}) = S(-D_i\, dC_i/dx + WC_i), \tag{A2}$$

$$= \frac{\bar{D}S}{LR\bar{T}} \left\{ -\Delta P_i + \frac{\bar{P}_i \sum_j^n m_j \Delta P_j}{\sum_j^n m_j \bar{P}_j} \right\}, \tag{A3}$$

where D_i and C_i are the diffusivity and the concentration of i-th gas component respectively, W is the laminar flow velocity, x the position parameter, and S the cross sectional area of the ampoule. $\bar{D}$ is the mean diffusivity of gaseous molecules which was calculated by using Lennard-Jones parameters in Appendix 3. L is the distance between the source and the growth zone.

$$\bar{T} = (T_g + T_s)/2, \tag{A4}$$

$$\bar{P}_i = (P_i^g + P_i^s)/2, \tag{A5}$$

ΔP_i is the pressure difference between the growth and source zones, which is regarded as a driving force for the transport. The transport rate (N) was calculated as follows,

$$N(\mathrm{kg/s}) = M_0 \times 10^{-3} \sum_{i=1}^{n} m_i J_i \tag{A6}$$

where M_0 is the molecular weight of ZnSe or $AgGaS_2$ and m_i is the number of Zn or Ag in the i-th gas component.

Under the condition of high vapor pressure and large cross-section of the growth ampoule, the mass transfer is modified by thermal convection, which is caused from the interaction between gravitational force and the gas density difference due to the temperature gradient. The gas flux and the transport rate are given by using the quantity $K^{(12)}$ as follows,

$$J_i^* = J_i(K+1), \tag{A7}$$

$$N^* = N(K+1), \tag{A8}$$

where

$$K = [A/(ScGr)^2 + B]^{-1}, \tag{A9}$$

where Sc and Gr are the Schmidt and the Grashof numbers, respectively, calculated in Appendix 3. The dimensionless quantities of $A = 6.95 \times 10^7$ and $B = 6.56 \times 10^{-2}$ were estimated for the ampoule geometry ratio (L/d) of $12.5^{12)}$ where d is the ampoule diameter.

3. Transport parameters

The transport parameters were calculated as follows[15-19] and shown in Figs. A1 and A2

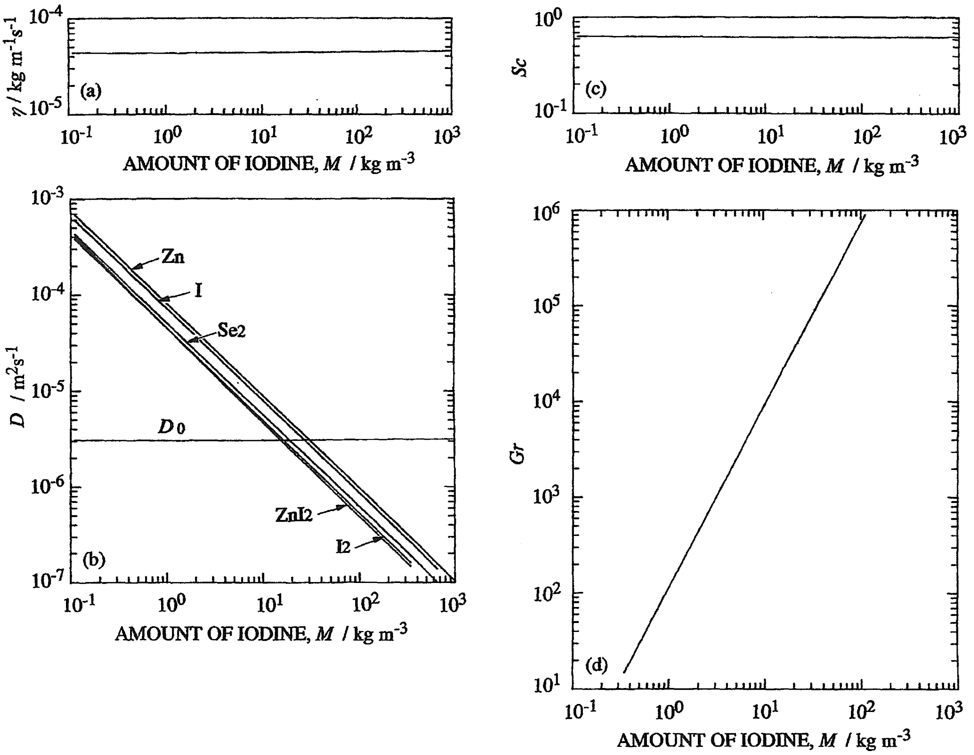

Fig. A1. The transport parameters of gas mixture as a function of amount of iodine in the transport system of ZnSe+I$_2$ at T_s=1098 K and ΔT=25K: (a) viscosity, (b) diffusivity, (c) Schmidt and (d) Grashof numbers.

for viscosity, diffusivity, Schmidt and Grashof numbers.

(i) Lennard-Jones parameters

The values of the Lennard-Jones parameters for the gaseous molecules taken from the literature[19] are listed in Table I and II with the thermodynamic data. When the values of power factor (ε/k) are not available, we estimated by using the approximate procedures as follows,

$$\varepsilon/k = 1.15T_b, \tag{A11}$$

$$\varepsilon/k = 1.92T_m, \tag{A12}$$

where T_b and T_m are boiling and melting temperatures in K, respectively. When Eqs. (A11) and (A12) give differing values of ε/K, the values are averaged. The difference between those values calculated by using the Eqs. (A11) and (A12) is recognized as small. Table I and II also lists σ_i the collision diameter of the molecule in m. In case of being unavailable, the values of σ_i were taken from those reported for the molecules having the similar molar weight.

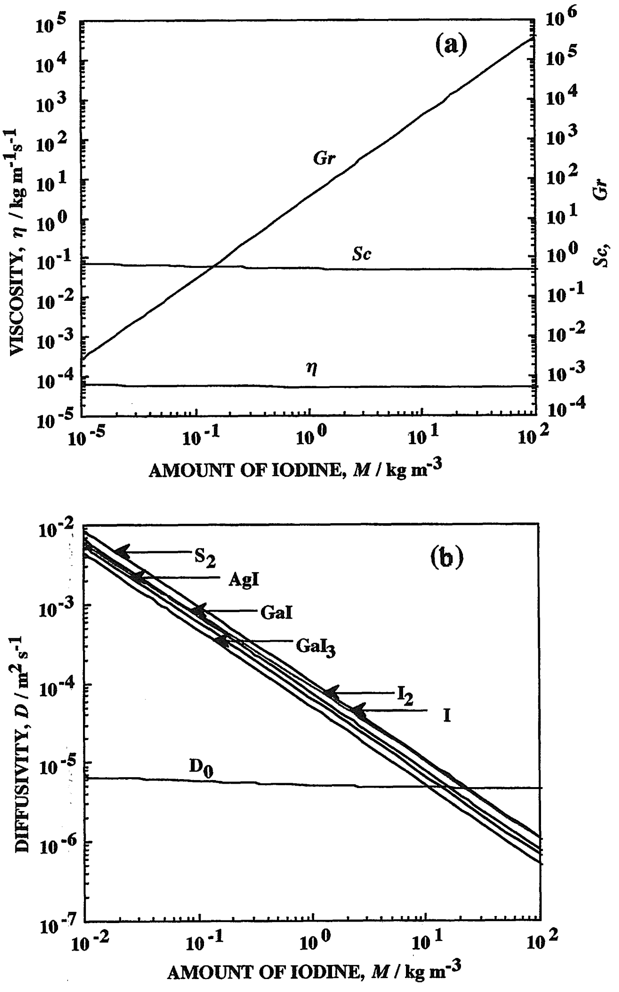

Fig. A2. The transport parameters of gas mixture as a function of amount of iodine in the transport system of $AgGaS_2+I_2$ at $T_s=1248$ K and $\Delta T=25$K: (a) viscosity(η), Schmidt (Sc) and Grashof(Gr) numbers and (b) diffusivities.

(ii) Viscosity of gases

The viscosity of nonpolar gases at low pressures is give as follows:

$$\eta_i=8.4411\times 10^{-25}(M_i \bar{T})^{1/2}/(\sigma_i^2\Omega_\eta), \qquad \text{(A13)}$$

where the collision integral of viscosity (Ω_η) is estimated from the table listed in terms of $k\bar{T}/\varepsilon$15). M_i is molar weight (kg) and η_i is in kg/(m s).

For the multicomponent gas mixture, the following formula is given,

$$\eta=\sum_{i=1}^{n}\frac{x_i\eta_i}{\sum_{j=1}^{n}x_i\Phi_{ij}}, \tag{A14}$$

in which

$$\Phi_{ij}=\frac{1}{\sqrt{8}}\left(1+\frac{M_j}{M_i}\right)^{-1/2}\left[1+\left(\frac{\eta_i}{\eta_j}\right)^{1/2}\left(\frac{M_j}{M_i}\right)^{1/4}\right]^2 \tag{A15}$$

n is the number of gas species in the mixtures; x_i and x_j are the mole fractions of species i and j; η_i and η_j are the viscosities of species i and j at the system temperature and pressure; and M_i and M_j are the corresponding molar weights.

(iii) Diffusivity

For the interdiffusivity D_{12} (in m^2/s) of two unequal gases 1 and 2, we have the following equation, which is strictly applicable for spherical monatomic gases:

$$D_{12}=5.9543\times10^{-24}\bar{T}^{3/2}(1/M_1+1/M_2)^{1/2}/(P\sigma_{12}{}^2\Omega_D), \tag{A16}$$

where $\sigma_{12}=(\sigma_1+\sigma_2)/2$ collision diameter in m, Ω_D collision integral for 1–2 mixture at dimensionless temperature $(T_{12}{}^*)$, the vales of which were taken from the table listed in terms of $(\varepsilon/k)_{12}$[15].

$$T_{12}{}^*=\bar{T}/(\varepsilon/k)_{12}, \tag{A17}$$

$(\varepsilon/k)_{12}=[(\varepsilon/k)_1(\varepsilon/k)_2]^{1/2}$ is the averaged intermolecular force parameter, in K; P is the sum of average pressures for 1 and 2 gases,

$$P=\bar{P}_1+\bar{P}_2 \text{ in Pa.} \tag{A18}$$

For the 1, 2,$\cdots$, n-component gas mixture, the diffusion coefficient of component 1 is expressed as follows:

$$D_{1,\mathrm{mix}}=(1-y_1)/[(y_2/D_{12})+(y_3/D_{13})+(y_4/D_{14})+\cdots+(y_n/D_{1n})] \tag{A19}$$

where D_{1i} is the diffusion coefficient of component 1 in the 1-i binary system.

$$y_i\equiv\bar{P}_1/\sum_i\bar{P}_i \tag{A20}$$

The $\bar{D}$ value was taken from the diffusivity of Se$_2$ or S$_2$, since the Se$_2$ or S$_2$ flux was considered to determine the transport rate of ZnSe or AgGaS$_2$ and the diffusivities of the gas species were almost comparable as shown in Fig. A1b and A2b where D_0 is diffusivity appeared in the equation,

$$\bar{D}=D_{X_2}\quad(\mathrm{X=Se\ or\ S}) \tag{A21}$$

$$\bar{D}=D_0(\bar{T}/273)^{3/2}/P_{\mathrm{total}}. \tag{A22}$$

(iv) Schmidt and Grashof number

The Schmidt Sc and Grashof number Gr are given as follows,

$$Sc = \eta/(\rho\bar{D}), \tag{A23}$$

and

$$Gr = d^3 g \beta \rho^2 \Delta T/\eta^2, \tag{A24}$$

where β is the thermal expansion coefficient equal to $1/\bar{T}$ for ideal gas and g gravitational acceleration$(=9.81\ \mathrm{m/s^2})$. ρ is gas density$(\mathrm{kg/m^3})$ given as follows,

$$\rho = \sum_{\mathrm{i}} [\bar{P}_{\mathrm{i}} M/(R\bar{T})], \tag{A25}$$

where R is gas constant$(=8.31451\ \mathrm{J\ mol^{-1}K^{-1}})$.

References

1) R. Nitsche: J. Phys. Chem. Solids, **17** (1960), 163.
2) T. Arizumi, T. Nishinaga: Jpn. J. Appl. Phys., **4** (1965), 165.
3) T. Arizumi, T. Nishinaga: Jpn. J. Appl. Phys., **5** (1966), 21.
4) S. Fujita, H. Mimoto, H. Takebe and T. Noguchi: J. Cryst. Growth, **47** (1979), 326.
5) E. Kaldis: *Crystal Growth, Theory and Techniques,* Vol. 1, ed by C. H. L. Goodman, (Plenum, New York, 1974), p. 49.
6) W. H. Honeyman, K. H. Wilkinson: J. Phys., **D4** (1971), 1182.
7) H. A. Chedzey, D. J. Marshall, H. T. Parfitt, D. S. Robertson: J. Phys., **D4** (1971), 1320.
8) Y. Noda, Y. Furukawa and K. Masumoto: *Memoirs of the Faculty of Science and Engineering, Shimane University,* Series A, Vol. 32, (1998), p. 1.
9) O. Kubaschewski, E. Ll. Evance and C. B. Alcock: *Metallurgical Thermochemistry,* 4th ed., (Pergamon Press, London, 1967), p. 267.
10) K. C. Miller: *Thermodynamic Data for Inorganic Sulfides, Selenides and Tellurides,* (Butterworth, London, 1974), p. 60.
11) E. Sirtle: Z. Naturforsch., **21a** (1966), 2001.
12) K. Klosse and P. Ullersma: J. Cryst. Growth, **18** (1973), 167.
13) F. C. Franck: J. Cryst. Growth, **46** (1979), 591.
14) Y. Noda, T. Kurasawa, H. Watanabe, Y. Furukawa and K. Masumoto: *Non-stoichiometry in Semiconductors,* ed. K. J. Bachmann, H.-L. Hwang and C. Schwab, (Elsevier, 1992), p. 63.
15) R. B. Bird, W. E. Stewart and E. N. Lightfoot: *Transport Phenomena,* (John Wiley & Sons, New York, 1960), p. 19, 495.
16) G. H. Geiger and D. R. Poirier: *Transport Phenomena in Metallurgy,* (Addison-Wesley Pub. Co. Inc., Massachusetts, 1973), p. 11, 463.
17) K. Sato: *Evaluation of Physico-chemical Constants* (in Japanese), (Maruzen, Tokyo, 1968), p. 77, 125.
18) S. Oh-e: *Estimation Methods of Chemical Properties for Engineers* (in Japanese), (Nikkan Kogyo, Tokyo, 1985), p. 229, 289.
19) R. A. Svehla: *NASA Technical Report,* **R-132,** (U.S.Government Printing Office, Washington D.C., 1962), p. 1.